Bulletin of Earth Sciences of Thailand

Hydrocarbon and Reservoir Mapping Using Seismic Simulated Annealing Inversion, in Southern Pattani Basin, Gulf of Thailand

Egi Ramdhani*

Petroleum Geoscience Program, Department of Geology,
Faculty of Science, Chulalongkorn University, Bangkok, 10330, Thailand
*Corresponding author email: egiramdhanim@gmail.com

Abstract

The research was conducted in southern Pattani Basin, Gulf of Thailand that is known as a mature hydrocarbon play. The sands reservoirs of sand A and sand B were studied by using seismic P-impedance inversion to image the oil-bearing reservoir distribution. Although several wells have been drilled, other areas haven't been proven to develop the reservoir due to a lack of wells drilled in the northern and southern areas. Therefore, this research conducted to mapping the distribution of oil-bearing sand at those areas. Rock physic analysis indicates that interest zone have low-density and can be discriminated against other lithology. Full-stack and partial stack seismic data were inverted producing absolute and relative impedance volumes which were compared to distinguish the best techniques for imaging the reservoir. Absolute impedance volume has more reliable results and is used to differentiate oil-bearing sand with other lithologies. According to rock physic and absolute p-impedance analysis, porous sand and different lithologies (tight sand and shale) have significant impedance contrast. Porous sand has low impedance value and the impedance of tight sand and shale fall in the high range. Multi-well blind tests show a reasonable match. Reservoirs distribution observed using horizon slices indicate sand A shows a large and broad reservoir zone that is hard to identify in the interest zone. The sand B is smaller and identified as alluvial fan deposited in the lacustrine environment. This research indicates that full-stack absolute impedance inverted volume can be used to identify oil-bearing sand distributions. Inverted volume cannot fully differentiate oil-bearing sand apart with wet-sand. However, in most cases, oil-bearing sand can be predicted.

Keywords: Post-stack seismic inversion, Simulated annealing inversion, Reservoir imaging, Pattani Basin, Gulf of Thailand

1. Introduction

The study area located in the Pattani Basin, Gulf of Thailand. Pattani is a mature hydrocarbon basin with proven reserves of oil and gas. This study will focus on the southern part of the Pattani basin which has oil discovered in Oligocene to Miocene age sandstone reservoirs. Typical reservoirs in the Pattani basin are sandstones deposited in the mainly fluvial depositional environment which have significant vertical and lateral change. Moreover, many of the reservoirs are below seismic resolution. Although most reservoirs in the Pattani Basin are controlled by structural traps that are associated with normal faulting, some stratigraphic traps are resulting in the difficulty of reservoir prediction.

An example of the complexity of the reservoirs is in Phoosongsee, et al., 2019, where several layers of tight sands have high density, high velocity and high p-impedance. This high p-impedance in some reservoirs results in uncertainty to discriminate sand and shale effectively. These conditions make characterizing the sandstone reservoir using seismic inversion a challenge.

P-Impedance inversion for reservoir imaging was studied in the same area by Tang-On, 2018. The study was focused on the area around the well location precisely in the central part of the research field. Due to the model-based p-impedance inversion on the research was not proved to differentiate oil-bearing sand and wet-sand, further study using the different technique were suggested.

The objective of this research is to improve seismic quality for understanding the distribution of reservoir also to discriminate the oil-bearing reservoir into other lithology using rock physic analysis. The main output of this research is an acoustic impedance map at the reservoir horizon with p-impedance contrast for

a better understanding of oil-bearing sand distribution.

2. Geology

The Pattani Basin is the deepest and longest of the rift basins in Thailand (Figure 1) and divided into three segments, which is the southern segment, central segment, and northern segment (Morley and Racey, 2011).

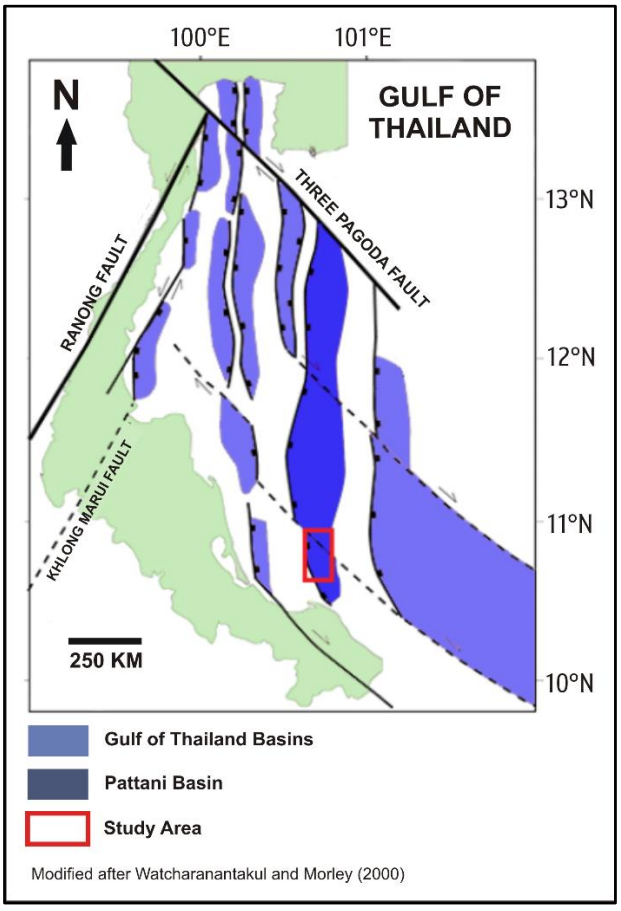

Figure 1. Regional tectonic map of the Gulf of Thailand (Modified after Watcharanantakul and Morley, 2000). The study area located in the southern part of the Pattani Basin, Gulf of Thailand.

The Pattani Basin divided into five stratigraphic sequences, and the target area was a part of sequence 1 that predominated by the late Oligocene claystone and limestone with 650 m thick. This sequence has very coarse to fine-grained sandstone are dominant in the lower part of sequence 1 and inferred to be deposited at lacustrine and alluvial-fan and fluvial-fan cannel (Charusiri and Pum-Im, 2009).

Buangam, 2011 identified that both structural and stratigraphic traps were found in the Pattani Basin. The structural traps are related to three-way dip closure against fault area, and fault traps itself. The stratigraphic traps mainly controlled by channel deposition and alluvial deposition.

3. Rock Physic Analysis and Seismic AI (Acoustic Impedance) Inversion

Rock physic analysis is used to establish parameters that can discriminate lithology and fluid within the reservoirs through the sensitivity test. This analysis can discriminate the hydrocarbon-bearing sand and the wet-sand, although in some cases, it was not proven due to data ambiguity. The parameters are P-wave velocity (Vp), density (ρ), P-impedance (Z), porosity (ϕ), resistivity (Rt) and water saturation (Sw) derived from measured log data.

Seismic inversion is the process of transforming seismic reflectivity and measured well data into a quantitative description of the subsurface. Seismic inversion is the backward modeling of seismic data to generate the stratigraphic model of the earth. The acoustic impedance (AI) or P-Impedance is defined as a result of P-Wave (Vp) multiplied by density (ρ). It is related to a normal incidence reflection and strongly related to the reflection coefficient.

Simulated annealing inversion is an inversion process that requires an initial model as an input. It is different input with color inversion, which does not require an initial model with macro model log parameters. This method is used to see a more accurate hydrocarbon distribution based on the distribution of AI value from the lateral view (Ginting et al., 2019).

4. Methodology

This study is focused on reservoir imaging using geophysical data at the interest zone at two sand bodies; Sand A and Sand B. Both sand body located below 5000 ft (1524 m) TVDSS with thickness average 39.25 m for sand A and 21.1 m for sand B. The reservoir imaging is using the seismic acoustic impedance for both absolute and relative impedance volume to detect possible reservoir at interest zone. Rock

physic analysis was used to identify the characteristic of the reservoir and to define the P-impedance cutoff of the interest zone that can discriminate the oil-bearing sand other lithology, including wet-sand. The p-impedance cutoff for oil-bearing sand identified by applying the resistivity cutoff at the linear regression line in p-impedance against resistivity cross plot. P-impedance cutoff for oil-bearing sand applied on the p-impedance map. The simplified workflow of the study shown in figure 2.

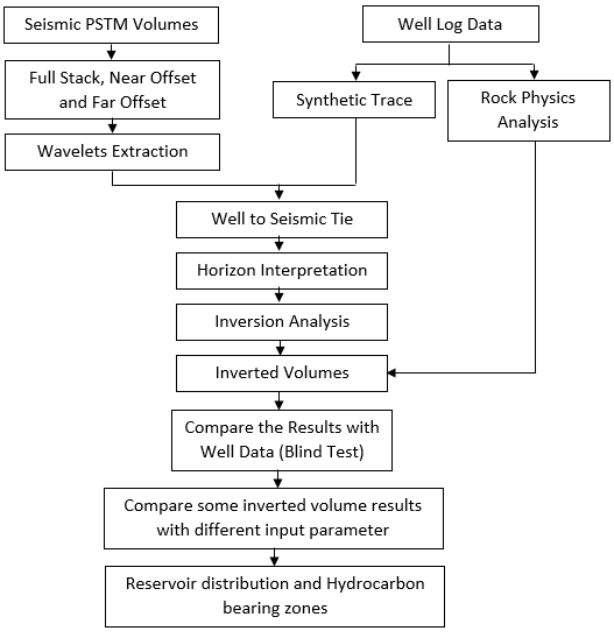

Figure 2. The simplified workflow of the research

5. Observations

5.1 General Seismic Observations

The main focus in this research is a reservoir known as reservoir Sand A and Sand B that deposited in sequence 1 at late Oligocene age, right above middle tertiary unconformity (MTU) that shown in figure 3. By looking at the seismic section in the crossline view, it is known that both sand A and sand B is pinched out against the middle tertiary unconformity.

Since it is known that sand A and sand B are deposited above middle tertiary unconformity (MTU) based on MTU marker correlated with the stratigraphic unit by Morley and Racey, 2011, then sand B is overlaid above sand A 30 ft into 85 ft based on available well data, some merged reflector of both sand observed at some seismic section, indicating that the sand layer might be below seismic resolution, this is caused by loss of higher frequency at this depth (1-1.5 s) as it known that the dominant frequency is quite low at 30 Hz (Fig. 4).

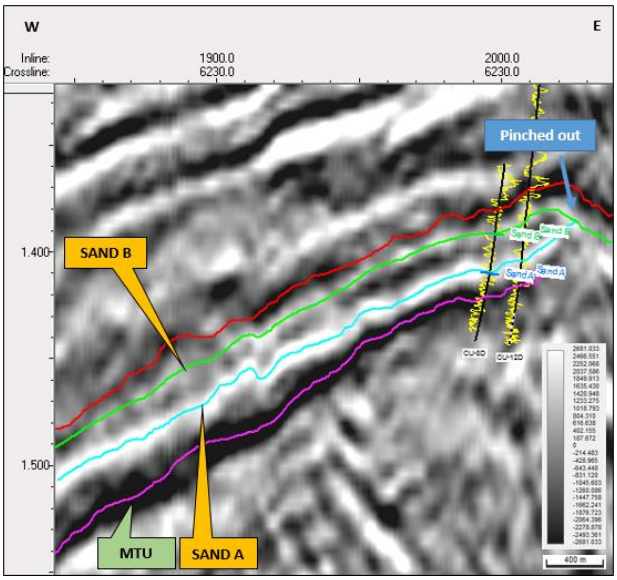

Figure 3. Seismic section from crossline 6230 showing pinched out point of both sand A and sand B. Both sand deposited above middle tertiary unconformity (MTU). Sandstone picked on peak due to increased velocity and density at water bottom showed by a trough, while sandstone is the reverse, decreasing Vp and density.

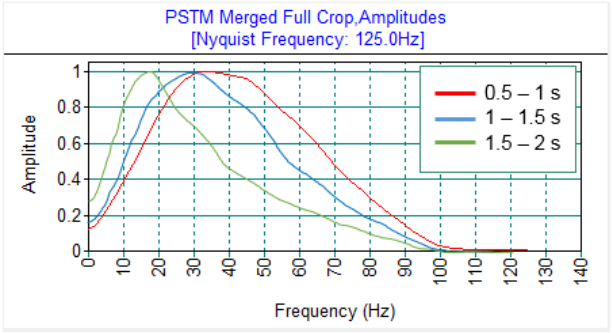

Figure 4. Comparison between survey spectrum at 0.5 s – 1 s (red line), survey spectrum at 1 s – 1.5 s at the reservoir zone (blue line), and survey spectrum at 1.5 s – 2 s (green line). It can be seen; the high frequency gradually lost due to increasing depth. This affecting tuning thickness higher and seismic resolution low.

5.2 Observation in Log Data

Figure 5 is showing log data in well CU-8D, where both sand A and sand B developed. This sand body identified as a low gamma-ray log value (low GR) with low NPHI and low

RHOB, causing separation indicating reservoir zone and high resistivity that support the assumption that the reservoir is filled by hydrocarbon (oil). Sand B is formed by a single sand body, and sand A is formed by three-layer sandstone interbedded with shale lithology. At the reservoir zone, effective porosity that calculated is showing a high number of PHIE at value range 20 percent to 30 percent, rarely reach more than 30 percent, indicating high available space of reservoir to accumulate fluid.

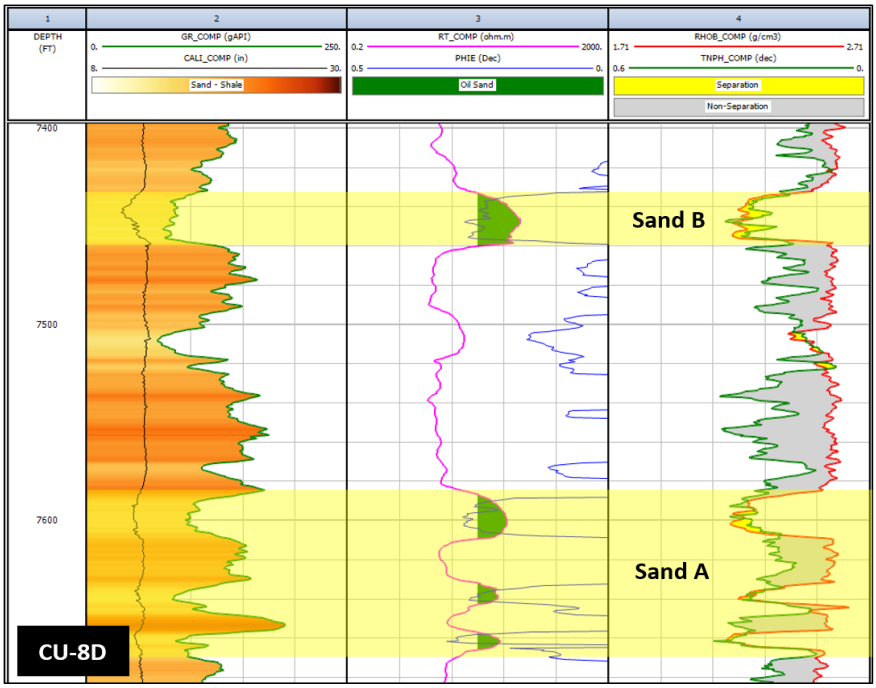

Figure 5. Well data view for well CU-8D showing both sand A and sand B developed and accumulated oil, with a high value of effective porosity (PHIE) and resistivity.

6. Interpretations and Results

6.1 Sensitivity and Rock Physic Analysis

Sensitivity and rock physic analysis were used to discriminate sands, also to discriminate oil sand and wet sand and their differences with other lithology. The challenge of this analysis is the presence of tight sand that makes ambiguity interpretation between shale and tight sand discrimination. Another challenge is, the data is not sensitive to fluid change within the reservoir, which can make oil-sand and wet-sand not fully differentiated. Clay volume is used to discriminate sand with other lithology (shale-related), where sandstone has low clay volume value below 35 percent, but other lithology indicated by a rapid increase of clay volume above 35 percent.

Figure 6 showing the cross plot for rock physic analysis from well CU-7D of p-wave, Density (RHOB), and p-impedance against clay volume (VCL) and P-wave, Density (RHOB) and p-impedance against each other. The black dashed line represents the clay volume cutoff at 35 percent value. A computed window is from top of sand B into the bottom of sand A. Figure 6A, where p-impedance was computed, at low-density sandstone, the p-impedance showing low value below 8000 m/s*gr/cc. At shally lithology, P-impedance showing high-value relative the same as high-density sandstone. Furthermore, figure 6B shows p-impedance, density, and p-wave combined. This shows that at low-density sandstone, which means a target zone as a reservoir, the p-impedance computed has low impedance value below 8000 m/s*gr/cc as a result low density (2.1 – 2.4 gr/cc) multiplied with low p-wave velocity (3000 – 3500 m/s), while in the high-density sandstone and shale, the p-impedance value was high due to a high density above 2.4 gr/cc and high p-wave velocity.

Trevena and Clark (1986) investigated the general diagenetic in the Pattani Basin. They found that porosity in sandstone can be reduced by cementation and compaction by several minerals such as quartz, dickite, kaolinite, and illite. This condition can be an explanation about why some low clay volume sandstone has high p-impedance value, high density, and high p-wave velocity value.

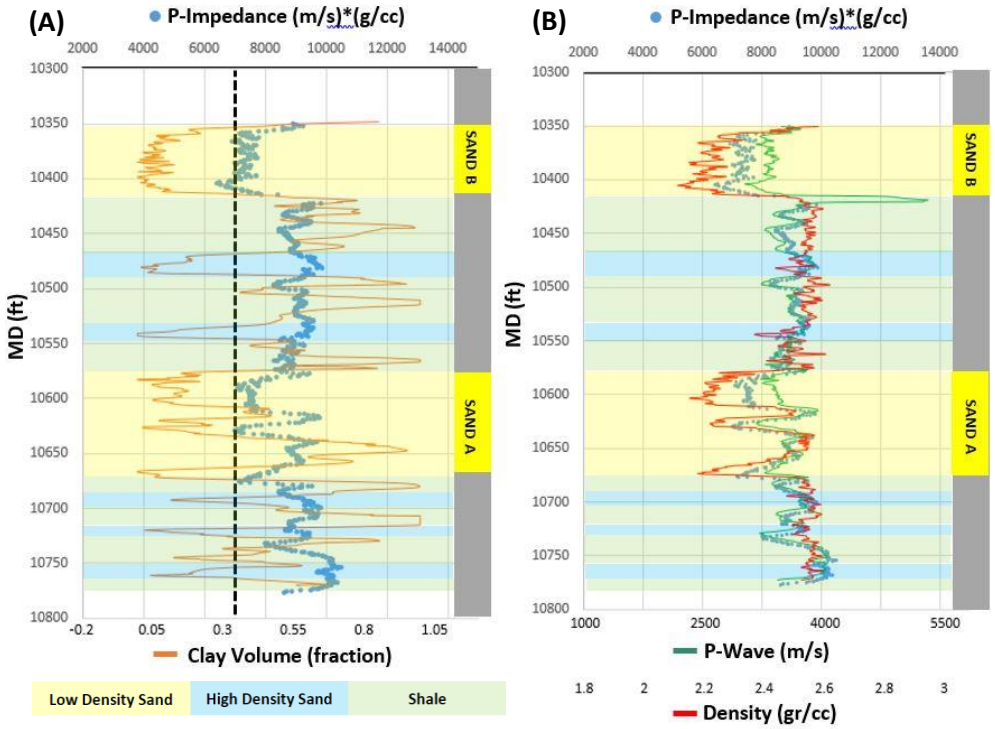

Figure 6. Cross-plots well CU-7D of (A) P-Impedance against clay volume; (B) P-wave, Density (RHOB), and p-impedance against each other. The black dashed line represents the clay volume cutoff at 35 percent. Low-density sandstone showed as low p-wave and p-impedance.

Figure 7 shows cross-plots from well CU-7D between resistivity (Rt) against P-impedance and effective porosity (PHIE) against P-impedance. At figure 7A, the cross-plot between effective porosity and p-impedance shows a linear relationship between these two parameters with a high correlation value. The higher effective porosity value, the lower p-impedance will be. By applying the effective porosity cutoff at 20 percent based on previous identification, it is resulting in the p-impedance cutoff at 8000 m/s*g/cc.

In figure 7(B), the p-impedance cutoff sought by applying the resistivity cutoff at 20 ohm.m based on previous identification (Fig. 5), where oil sand will have resistivity higher than 20 ohm.m. It is revealed that the p-impedance cutoff slightly higher than PHIE and p-impedance cross-plot at 8200 m/s*g/cc. Moreover, since the main focus at this research is trying to discriminate oil sand and wet sand, the resistivity value is more representative of the fluid within the reservoir than effective porosity (PHIE). The p-impedance cutoff based on resistivity against p-impedance are used for the further result.

However, it is found that low p-impedance value below the cutoff at 8200 (m/s)*(g/cc) also appear in low resistivity value below resistivity cutoff, remarked as red dashed line. This condition is an effect of wet-sand and delivers to the conclusion that p-impedance actually cannot fully differentiate oil-bearing sand and wet-sand. But, it still can separate porous sandstone (low-density sand) with tight sandstone and shale effectively. However, since the wet sand data that plotted are nearly cutoff line, the cutoff range for oil-bearing sand

changed into range 8000 into 8200 (m/s)*(g/cc). With high confident level at cutoff at 8000 (m/s)*(g/cc), and the possibility of wet sand found at range 8000 into 8200 (m/s)*(g/cc), but oil-bearing sand also can be found at this range.

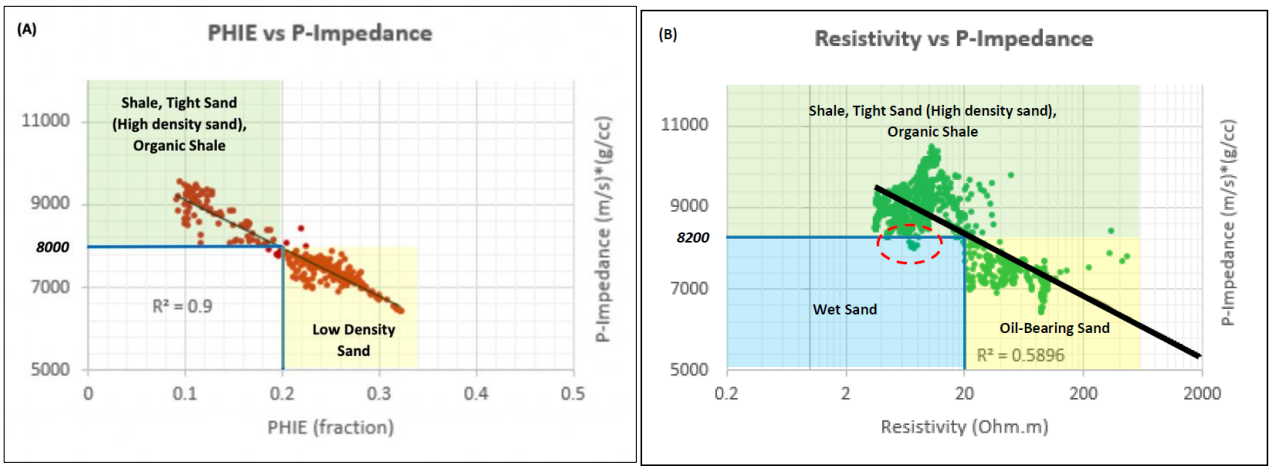

Figure 7. Cross-plots well CU-7D between (A) resistivity (Rt) against p-impedance and (B) effective porosity (PHIE) against p-impedance. The blue line is showing the cutoff of both parameters in each cross-plots. p-impedance cutoff based on PHIE and Resistivity cutoff. These show the higher porosity and resistivity, the lower p-impedance value. Red dashed circle is overlapped data indicating wet-sand.

6.2 Seismic Inversion

Seismic inversion generated using simulated annealing inversion module at 3D PSTM full-stack volume, 3D Far offset volume, and 3D Near offset volume using well CU-7D, CU-12D, and CU-15D. A blind test of inverted volume on seismic section 3D PSTM full-stack data volume with 3 different well input shown in figure 8 for absolute impedance contrast. The relative impedance result shows the same pattern. However, due to lack of low-frequency input, relative impedance is less reliable than the absolute impedance inverted volume that requires the macro model as an input for the low-frequency model. Thus, interpretation based on absolute impedance inverted volume was used.

Quality control for the multi-well blind test is using well CU-8D, CU-12D, and CU-4ST for inverted volume by well CU-7D. Multi-well blind test using well CU-7D, CU-8D, and CU-4ST for inverted volume by well CU-12D and multi-well blind test using well CU-7D, CU-12D, CU-8D, and CU-4ST for inverted volume by well CU-15D. Figure 8, the absolute impedance result, it can be seen that inverted volume by well CU-7D, can separate sand A and sand B but has unclear lateral continuity due to poor match response between Gamma-ray log and inverted volume showed as circled area. However, the blind test matched between Gamma-ray log data and the inverted seismic data volume. Inverted data by well CU-12D also can separate sand A and sand B with the continuity clearer than the previous result in the same area. The blind test also matches between the Gamma-ray data and inverted volume result. The other inverted result by well CU-15D, sand A and sand B are separated but has low lateral continuity among the other. The multi-well blind test result also shows an unreasonable match. By this result, the best-inverted volume is the same as relative impedance contrast, made by using well CU-12D, followed by well CU-7D, and the last is well CU-15D.

Based on this response in multi-well blind test analysis, it concluded that, in 3D PSTM Full Stack volume, the best-inverted volume is a volume which generated using well CU-12D. Multi-well blind test analysis also applied at another inverted volume using near offset 3D PSTM data and far offset 3D PSTM data using well CU-12D as an input.

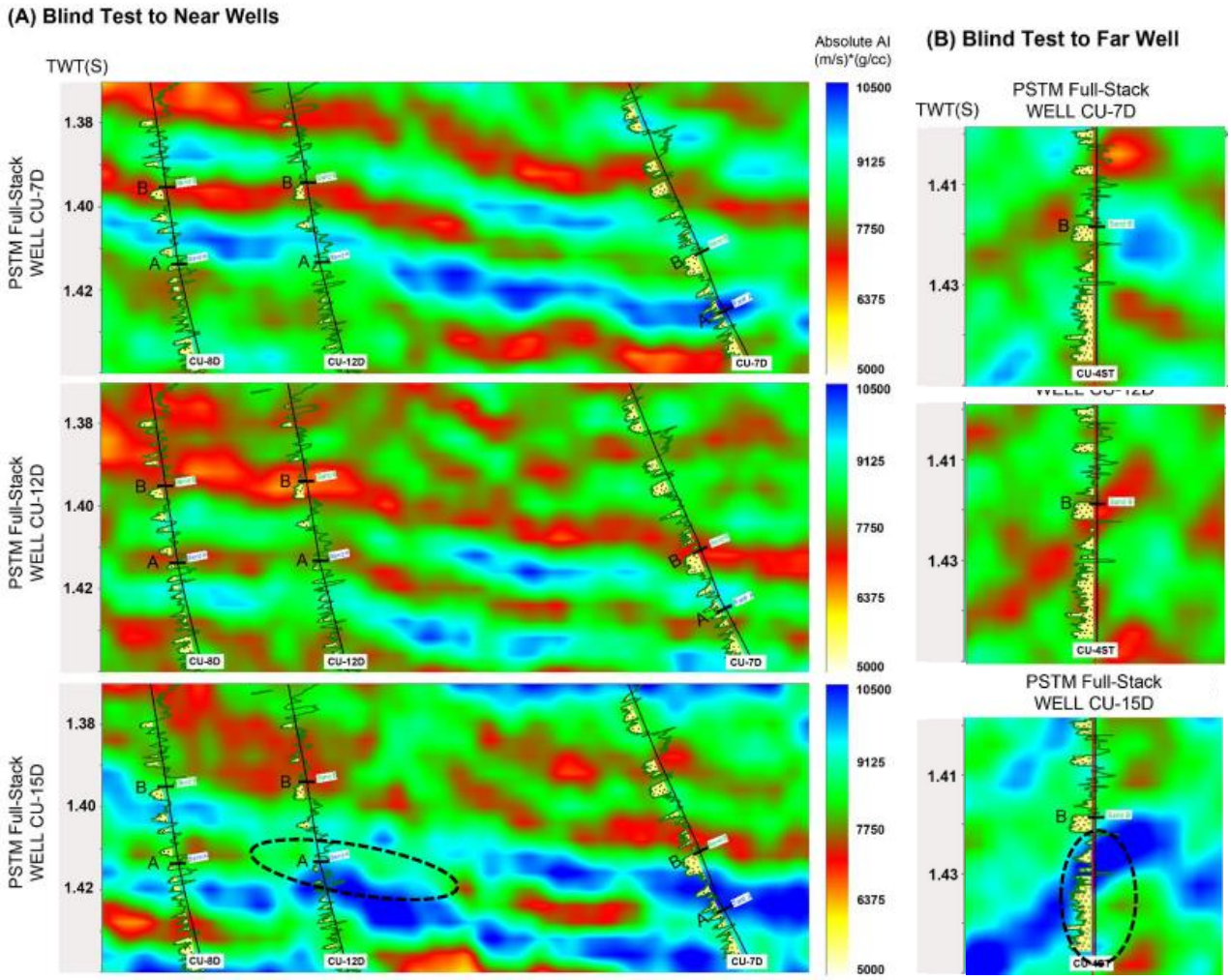

Figure 8. Cross-section for the multi-well blind test in absolute impedance volume generated by each well CU-7D, CU-12D, and CU-15D with full-stack seismic volume. Gamma-ray showed in green line with yellow shading indicating sandstone. (A) Blind test to the near well and (B) Blind test to the far well. Result by well CU-7D and CU-12D shows reasonably match and inverted volume by well CU-15 has the least match.

Figure 9 showing an inverted result generated using well CU-12D at three different 3D PSTM input volumes, the full-stack volume, near offset volume, and far offset volume with absolute impedance output. Blind test analysis using the same parameter as before, the gamma-ray log plotted as a green curve with yellow shading indicating sandstone and well tops showed along the borehole. Well logging analysis mentions that the near wells that used in the blind test are a productive well for both sand A and sand B. In contrast, far well (CU-4ST) only productive well for sand B, moreover, the inverted volume response should have low impedance response that would be matched with low gamma-ray value since reservoir area is a low-density sandstone with low shale content. Full-stack inverted volume in figure 9 shows a good and reasonable match between absolute impedance volume with the gamma-ray log curve. It also has clear lateral continuity in both sand A and sand B reservoir. Near offset inverted volume giving a good match at sand B reservoir zone but giving an unreasonable match at sand A at the circled area with low lateral continuity but still showing its lateral distribution. Far offset inverted volume giving the least reasonable match at sand A and sand B (circled area), also, has unclear lateral continuity in both target zone due to thick amplitude in far offset volume. Thick amplitude occurs due to far offset data lost its higher frequency.

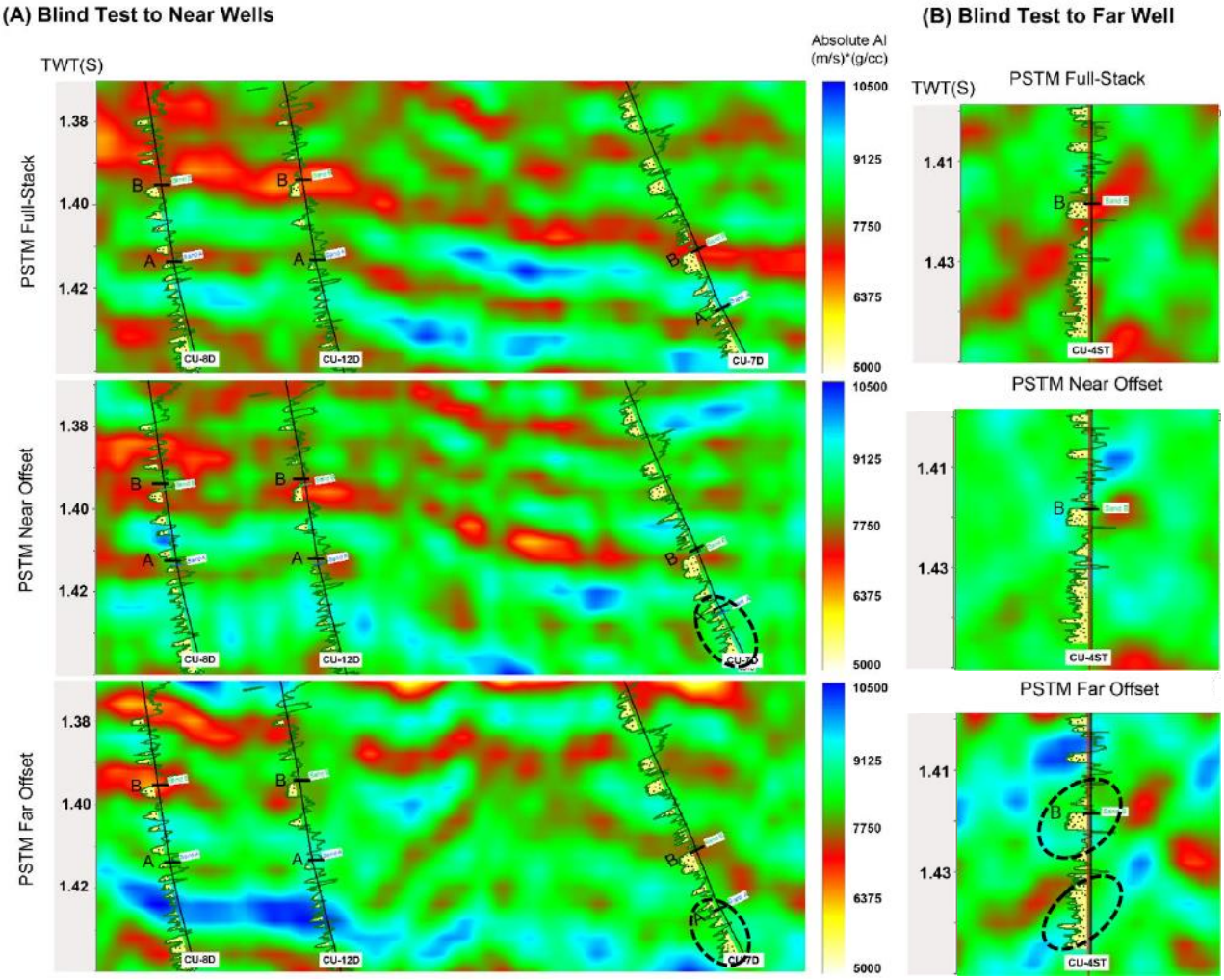

Figure 9. Cross-section for the multi-well blind test in absolute impedance volume generated by well CU-12D with full-stack, near offset, and far offset seismic 3D volume. Gamma-ray shown in green line with yellow shading indicating sandstone. (A) Blind test to the near well and (B) Blind test to the far well. Full-stack and near offset inverted volume giving the reasonably match. Far offset inverted volume has the least match due to the thick amplitude of reflection in the target zone.

Based on this interpretation, it is known that inverted volume using full-stack data and near offset data giving a reasonably match at the blind test and giving clear lateral continuity response at sand A and sand B reservoir. Meanwhile, far offset inverted volume giving low reasonable match due to thick amplitude at seismic input. Another reason is the original well data has near offset feature which do not match with far offset, seismic well tie with far offset data may help, but due to many changes in synthetic, it may lead to misinterpretation. To avoid this and increase the confident level of interpretation, full-stack inverted volume was used because full-stack inverted volume giving the best reasonable match for this research.

Overall, relative impedance and absolute impedance inverted volume that generated using well CU-12D show a reasonable match in the seismic section at full-stack volume and near offset volume. Far offset inverted volume has the least reasonable match that can lead to misinterpretation. A least reasonable match can be due to thick amplitude at low-frequency data and critical angle effect. However, 3D PSTM full-stack inverted volume has the best reasonable match at this research with a good match and clear lateral continuity at the inverted cross-section. Thus, horizon slice in full-stack inverted volume at both sand A and sand B can be displayed to analyze the distribution of oil-bearing sand.

Figure 10(A) and (B) show the horizon slice in the relative impedance at sand A and sand B. Both sand A and sand B believed pinched out against the middle tertiary unconformity (MTU). This pinch out creates onlap for sand A and sand B. white zone is an identified area where sand A and sand B did not develop. 11 well data available in this research, this well data confirmed that sand A did not develop in the white area due to pinched out effect. Meanwhile, 11 available well drilled against sand B cannot confirm the white zone where sand B identifies undeveloped since there is no well drilled at the white area of sand B. Thus, the identification of onlap in sand B based on seismic section.

At this horizon slice, the low-density sand indicated as a low value of impedance highlighted as dark red into bright yellow color with impedance cutoff at 8200 (m/s)*(g/cc). There is still a possibility of wet-sand appear in this cutoff. Thus, the oil-bearing sand cutoff is applied at slightly lower than low-density sand, at 8000 (m/s)*(g/cc). Low-density sand A distribution is characterized by low absolute impedance value based on rock physic analysis.

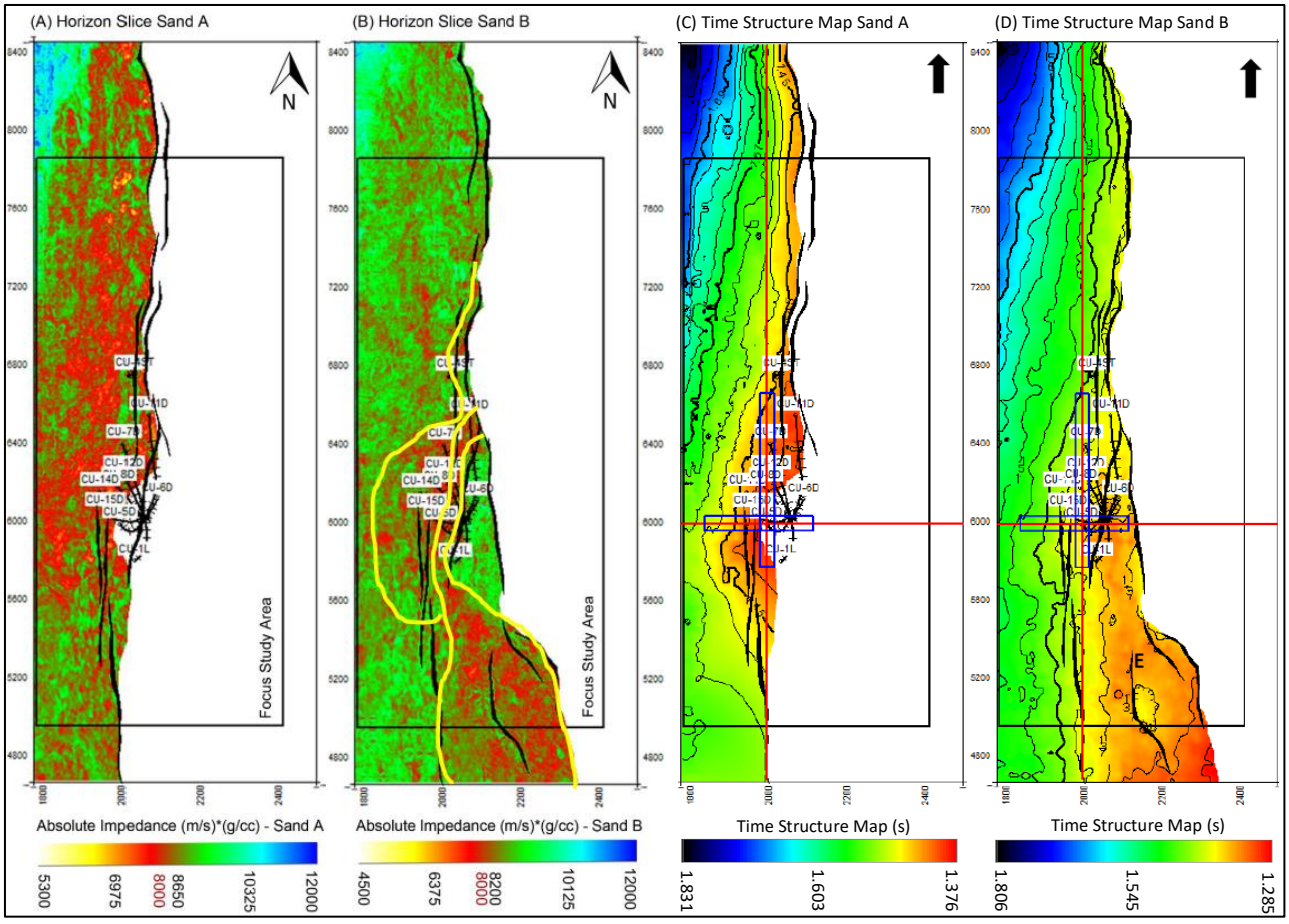

Figure 10. Absolute impedance contrast (A) Horizon slice sand A, (B) Horizon slice sand B. Dark red into bright yellow indicating oil-bearing sand. The yellow line was representing the border of the interest zone, concludes the depositional environment at the alluvial fan of the lacustrine. On the other hand, time structure map of research filed (C) sand A and (D) Sand B, with focus area highlighted with black box. White area indicating sand A and sand B not developed due to pinched out effect.

The cutoff for low-density sandstone, as mentioned before, cannot discriminate oil-bearing sand and wet sand effectively. However, by setting the cutoff at 8000 (m/s)*(g/cc), it still can differentiate the oil-bearing sand and wet-sand. Oil-bearing sand, which distributed widely in almost all parts of sand A in the research area, has low impedance value below 8000 (m/s)*(g/cc) indicated by dark red color into bright yellow. In the focus study area, the

northern area seems to accumulate more hydrocarbon than the southern area. Thus, this shows that the northern area has more exploration interest than the southern area. Oil bearing sand B distribution also characterized by low absolute impedance value below 8000 (m/s)*(g/cc). Looking at figure 10(B), the interest zone distributed at the southern part of the research area, combined interpretation between impedance map with time structure map (Fig. 10(D)), it is known that there is a possibility hydrocarbon in southern area accumulated in the high closure against fault in sand B.

The northern area at focus study has less potential, while in the southern area, oil-bearing sand found. Thus, for sand B, the southern area has more interest than the north area. Overall, looking at the entire distribution of oil-bearing sand based on absolute inversion volume, sand A is more interesting than sand B. Sand B indicated more water-bearing sand. However, some interest zone also found in high closure in the south area. In the northern area, there is no well-developed oil-sand due to a lack of trap.

7. Discussions

The post-stack time migration (PSTM) data in full-stack and partial stack volumes are suitable to run an inversion for this dataset. The inversion techniques can be used to distinguish the oil-bearing sand in both sand A and sand B based on the objectives of this research by applying the cutoff at 8000 (m/s)*(g/cc) at the absolute impedance inverted volume. However, the impedance value at range 8000 – 8200 (m/s)*(g/cc) cannot fully differentiate oil-bearing and wet-sand due to overlapped data at rock physic analysis (Fig. 7).

Full-stack and partial stack inverted volume were better to improve the imaging of the interest zone in the study area compared with original seismic volumes. However, the inverted volume that generated using far offset seismic data has the poorest result. And the inverted volume that generated using full-stack seismic data shows the best match with multi-well blind test analysis, both with the near neighbor wells and the far well. This condition occurs due to far offset data contain more low-frequency data compared to full-stack and near offset data. This was causing the reflection at seismic data thicker due to lower frequency. Based on these results, inverted volume using full-stack seismic 3D data used to differentiate oil-bearing sand and with other lithology, including wet sand.

Absolute acoustic impedance shows better results for imaging the reservoir of oil-sand than relative impedance contrast due to absolute impedance contain low-frequency data that resulting in more reliable results, whereas relative impedance lacks it. In most cases, absolute acoustic impedance can discriminate oil-bearing sand zone with other lithology, including wet sand zone.

Figure 11 showing an absolute impedance map nearby the available well data. Yellow circle indicating oil-bearing sand based on well logging data analysis and well completion report, the light blue circle indicating wet sand or no pay develop and grey circle indicating the sand did not develop at that area. Looking at horizon slice of the absolute impedance of sand A in figure A, the figure shows 7 wells drilled in dark red into light yellow color impedance indicating oil-bearing sand, and another 3 wells drilled at an area where sand A not developed. Moreover, these results give a good match between well logging analysis and impedance analysis where 10 wells out of 10 are matching. Referring to well logging analysis in figure 5, sand A and sand B at well CU-8D identified as oil-bearing sand while sand B identified as wet-sand. Then in figure 11, both of these information matched with impedance value. Figure B that represents the absolute impedance at sand B, shows that 6 wells being drilled at dark red into yellow color indicating oil-bearing sand, another 5 wells drilled at green color indicating wet sand or no pay. Based on well logging analysis, it is known that well CU-14D is oil-bearing sand, but the impedance result showing it is drilled at wet sand zone at high impedance value shows as a green color, so it did not match. This is due to the capability of absolute impedance that cannot fully differentiate oil-bearing sand and wet-sand at a medium value of the impedance (8000 –

8200 (m/s)*(g/cc)) where CU-14D being drilled. At that impedance range, the interpretation can be both oil-bearing sand and wet-sand (see Fig. 7). It leads into a poor sensitive parameter to discriminate wet-sand and oil-sand. Moreover, at sand B, it is found that there are 10 wells out of 11 that match. Sand B in well CU-4 and CU-1L believed located below oil-water contact and causing a wet sand zone, and in well CU-6D believed as a not well-developed sand causing no pay zone. By this result, it proved that the p-impedance can mostly differentiate oil-bearing sand with other lithology, including wet-sand.

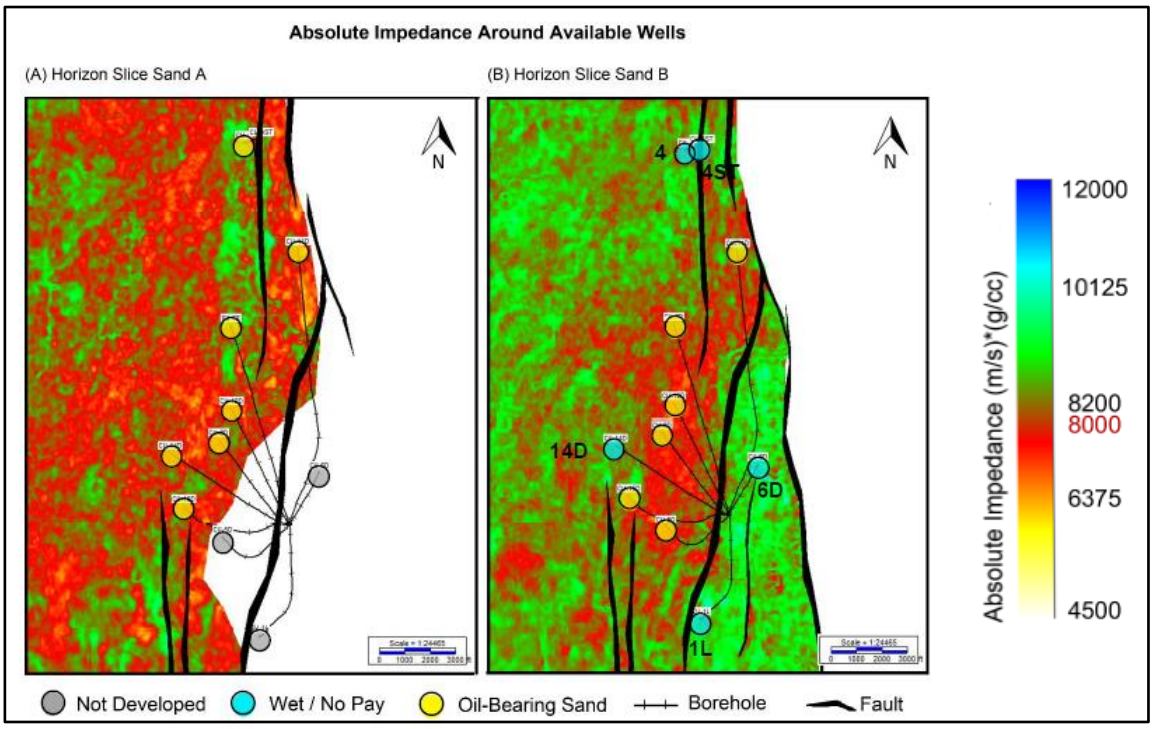

Figure 11. Absolute acoustic impedance map nearby the available well data at the research area. (A) All available wells, 10 out of 10 wells, match with the absolute p-impedance result at sand A. (B) 10 out of 11 wells match with the absolute p-impedance result.

Overall, data and results of this research implied a complex depositional environment where sand A and sand B being deposited. Based on Morley and Racey, 2011, both sandstones were deposited at the late Oligocene age as a sequence 1 of the Pattani Basin. And referring to Phoosongsee, et al., 2019, late Oligocene age has a majorly lacustrine depositional system. This is proved at the absolute impedance in horizon slice sand B, where interest zone at low impedance value creating a body shape of sand, marked with a yellow line in figure 10(B). The body shape interpreted as an alluvial fan of a lacustrine environment. This argument also supported by a well completion report that mentions the sand and sand B, part of the lower reservoir section, deposited in lacustrine or fluvial environments.

8. Conclusions

The objectives of this research are to understand the distribution of reservoir also to discriminate the oil-bearing sand into other lithology using rock physic analysis in the target of the research area. From these objectives, the rock physic analysis and seismic PSTM inversion were applied both in full-stack data and partial stack data. Conclusions are summarized below;

- Lithologies, fluids within the reservoir, and compaction affect the density value and P-wave. Moreover, it is affecting P-impedance value.
- Rock physic analysis at rock physic cross-plot shows that P-impedance cannot discriminate high-density sands with shales. However, low-density sand as the main focus

for this research can be differentiated with shale because it has an obvious p-impedance value contrast.

- Absolute P-impedance inverted volume has a better result in imaging the distribution of oil-bearing reservoir than relative p-impedance inverted volume.
- Absolute P-impedance inverted volume for full-stack data and near offset data mostly can be used to identify the oil-bearing sand and confirmed by blind test wells. However, far offset P-impedance inverted volume is not appropriate to use for this data set.
- Full-stack absolute P-impedance inverted volume has the best match with available wells. The success rate is 10 wells out of 10 for sand A and 10 wells out of 11 for sand B.
- Sand distribution interpretation shows alluvial fan form at sand B with a separated fan. While sand A has a broader and larger oil-bearing reservoir and cannot interpret the depositional form due to an unclear pattern, however, both sand A and sand B believed to be deposited at the lacustrine environment.
- Trap for sand A and sand B are likely associated with a structure (three-way dip closure against fault and faults) also stratigraphic traps.

9. Acknowledgement

I would like to express my gratitude towards my supervisor, Mr. Angus John Ferguson, for his enthusiastic support, invaluable advice and ideas, and his generous assistance throughout the research. Besides, I also would like to extend my sincere appreciation to PTT Exploration and Production Ltd. for offering me the opportunity to pursue my Master of Science in Petroleum Geoscience, Chulalongkorn University. My sincere thanks to KrisEnergy Ltd. for providing me the company's data needed for the research. Many thanks to Petroleum Geoscience Program lecturers and staffs for precious knowledge, support, and co-operation throughout the year.

10. References

Buangam, J. 2011. The stratigraphic trap in the Benchamas field, Pattani basin, Gulf of Thailand. *Bulletin of Earth Sciences of Thailand*, v. 4, p. 46-52.

Charusiri, P., and Pum-In, S. 2009. Cenozoic tectonic evolution of major sedimentary basin in central, northern, and the Gulf of Thailand. *Bulletin of Earth Sciences of Thailand*, v. 2, p. 40-62.

Ginting, H. B. R., Firmansyah, M., Ariansyah M. R., Aswad, S., and Siregar, D. R. 2019. Reservoir characterization using acoustic impedance seismic inversion method and seismic attribute in the "RST" field of the Taranaki basin, New Zealand. *Proceedings Indonesian Petroleum Association*, Jakarta, Indonesia, No. IPA19-SG-41.

Morley, C. K., and Racey, A. 2011. Tertiary stratigraphy, in MF Ridd, A. J. Barber and M. J. Crows, eds., The geology of Thailand. *Journal of Geological Society of London*, p. 223-271.

Phoosongsee, J., Morley, C. K., and Ferguson, A. J. 2019. Quantitative interpretation of seismic attributes for reservoir characterization of early-middle Miocene syn- and post-rift successions (Songkhla basin, Gulf of Thailand. *Journal of Marine and Petroleum Geology*, No. 109 (2019), p. 791-807.

Tang-On, A. 2018. The use of inversion volumes for reservoir imaging, CU field, Gulf of Thailand. Unpublished M.Sc. thesis, The Department of Geology, Faculty of Science, Chulalongkorn University.

Trevena, A. S., and Clark, R. A. 1986. Diagenesis of sandstone reservoirs of Pattani Basin, Gulf of Thailand. *The American Association of Petroleum Geologists Bulletin*, v.70, No.3, p. 299-308.

Watcharanantakul, R., and Morley, C. K. 2000. Syn-rift and post-rift modeling of the Pattani basin, Thailand: evidence for a ramp flat detachment. *Journal of Marine and Petroleum Geology*, v. 17 (2000), p. 937-958.